Article:
Wang, J.B., Wang, W.Y., Jewell, G.W. et al. (2002) A low-power, linear, permanent-magnet generator/energy storage system. IEEE Transactions on Industrial Electronics, 49 (3). pp. 640-648. ISSN: 0278-0046

https://doi.org/10.1109/TIE.2002.1005391

A Low-Power, Linear, Permanent-Magnet Generator/Energy Storage System

Jiabin Wang, *Member, IEEE*, Weiya Wang, Geraint W. Jewell, and David Howe

***Abstract*—This paper describes the design, analysis, and characterization of a linear permanent-magnet generator and capacitive energy storage system for generating electrical power from a single stroke of a salient-pole armature. It is suitable for applications that require relatively low levels of electrical power, such as remote electronic locks. An electromagnetic analysis of the generator is described, and a design optimization methodology for the system is presented. Finally, the performance of a prototype is validated against measurements.**

***Index Terms*—Generators, linear machines, permanent-magnet generators, power conversion.**

I. Introduction

THERE IS A growing demand in various market sectors for the reliable and remote provision of low levels of electrical power (<5 W), e.g., to supply electronic circuits in security locks data logging/telemetry systems. In many situations, on-board power generation is preferred to the use of batteries, which have a number of attendant problems, in that they contain toxic and corrosive materials, have a limited lifetime, and need regular maintenance [1], [2]. Further, there are situations in which a loss of power may be inconvenient, e.g., a remote electronic security device, or result in a breach of health and safety regulations, e.g., when monitoring operator use of machinery. A commonly available form of mechanical input energy is linear motion, which may be a reciprocating motion due to the vibration of a structure or machinery [3], or a single linear movement due, for example, to the pressing of a switch or the insertion of a key. Although such linear motions can be converted to rotary motion, by means of racks and pinions or cams, linear generators are often preferred, since they are simpler [4], [5], have a superior efficiency, and are more reliable [6], [7].

This paper is concerned specifically with the design of a system for generating and storing electrical energy from a single linear movement, to supply a remote electronic locks or an identification device such as fingerprint recognition systems, for example. In such applications, the generator may be idle for extended periods of time, until an operator inserts a key or presses a push-button. During the transient operating period, the generator charges an energy storage capacitor, which subsequently supplies the associated electronic circuitry.

Manuscript received March 26, 2001; revised December 25, 2001. Abstract published on the Internet March 7, 2002. This work was supported by the U.K. Engineering and Physical Sciences Research Council (EPSRC).

J. Wang, G. W. Jewell and D. Howe are with the Department of Electronic and Electrical Engineering, University of Sheffield, Sheffield, S1 3JD, U.K. (e-mail: g.jewell@sheffield.ac.uk).

W. Wang is with the Ultralab, Anglia Polytechnic University, Chelmsford, CM1 1LL, U.K.

Publisher Item Identifier S 0278-0046(02)04919-5.

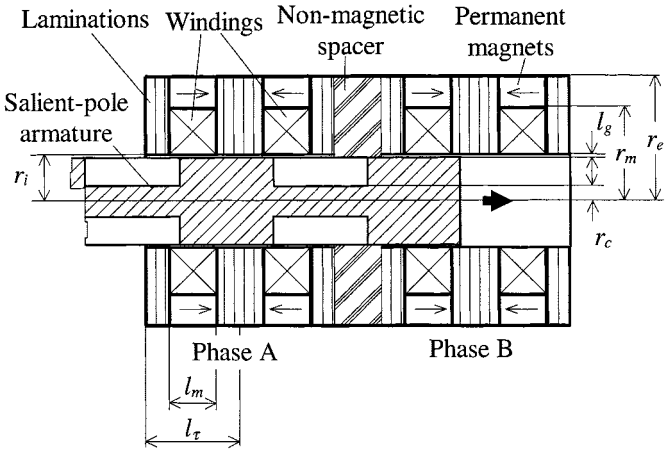

Fig. 1. Schematic of two-phase tubular permanent-magnet generator.

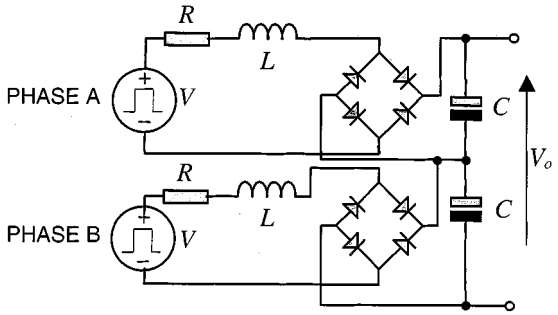

Fig. 2. Rectification and energy storage circuit.

The basic configuration of the linear generator that is under consideration is shown in Fig. 1, while Fig. 2 shows the associated power conditioning circuit. The generator is a two-phase tubular device, the stator having both permanent magnets and coils, while the moving armature is a simple salient iron core. The rectified output of the generator charges the capacitors to store the generated electrical energy. As demonstrated in [8], the circuit arrangement in Fig. 2 results in the best performance from a two-phase generator.

The axially magnetized permanent magnets and the laminated pole-pieces in the stator produce an essentially radial air-gap field. The stator winding flux linkage is modulated by the linear movement of the armature, and generates an induced electromotive force (EMF). It will be noted that generators of this type are often described as either "flux-switching" or "hybrid permanent-magnet" generators, so as to distinguish

them from more conventional topologies in which the permanent magnets are located on the moving armature. When the armature is removable, for example, if it acts as the key for a security system, the utilization of the generator is inevitably compromised since the armature can only be inserted from one end. Thus, the coils of phase *B* in Fig. 1 would be active only during the latter half of the stroke. When the armature is not removable, for example if it is integrated into a "push-button," the utilization of the generator can be improved significantly by employing an armature which is longer than the stator, such that the coils of both phases are fully active throughout the complete stroke.

One potentially important practical advantage of "flux-switching" generators is that the armature will not retain any significant remanent magnetization when the armature is removed. Thus, it would be suited to applications such as security locks, which could not tolerate a removable permanent-magnet polarized armature, since it may attract ferrous material, corrupt credit cards, etc. However, one potentially undesirable feature is the existence of cogging, which although not directly compromising the power capability, may cause significant velocity variations during the stroke, and affect the tactile "feel" of the device. However, the cogging force can be minimized by optimizing the width of the nonmagnetic spacer which separates the two phases [8], [9]. If the armature is removable, however, the extent to which the cogging force can be reduced is limited, particularly over the initial half of the stroke.

It will be noted that although the paper is concerned with a two-phase generator in which each phase comprises a two-coil module as shown in Fig. 1, a generator in which each phase has a number of such modules may be better suited to the available space envelope. However, for applications in which the armature is removable, this would further compromise the utilization of the windings.

II. Design

In order to illustrate the design synthesis methodology, the following performance specification has been addressed:

axial stroke: 48 mm;
average speed: 0.3 m/s;
stored energy: 3 mJ.

A detailed knowledge of the magnetic field distribution as a function of armature position is a prerequisite for performing design optimization of both the generator and the associated power conditioning circuit. Two analysis techniques are employed: a lumped equivalent magnetic circuit approach and magnetostatic finite element analysis, the former facilitating the rapid assessment of a large number of potential designs, while the latter facilitates design refinements and ensures that the field distribution is calculated to the required accuracy.

A. Lumped Magnetic Circuit Analysis

An equivalent magnetic circuit for the generator is established by making judicious assumptions regarding the predominant flux paths within the device. The equivalent circuit reluctances

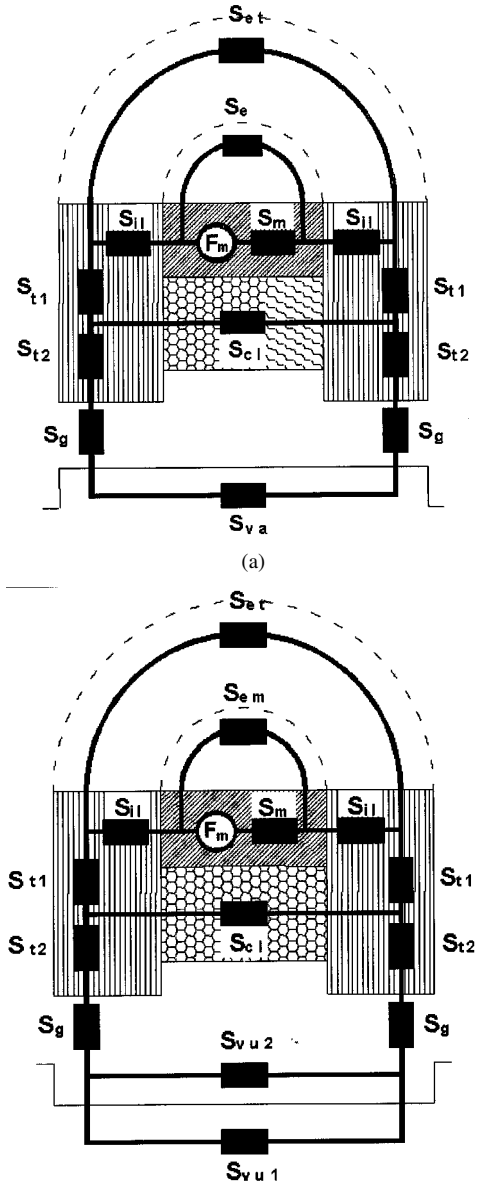

Fig. 3. Lumped magnetic circuits.

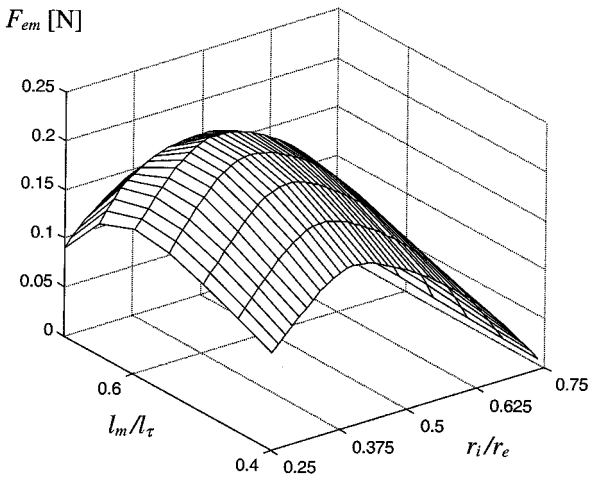

Fig. 4. Electromagnetic force as a function of the dimensional ratios r_i/r_e and l_m/l_τ.

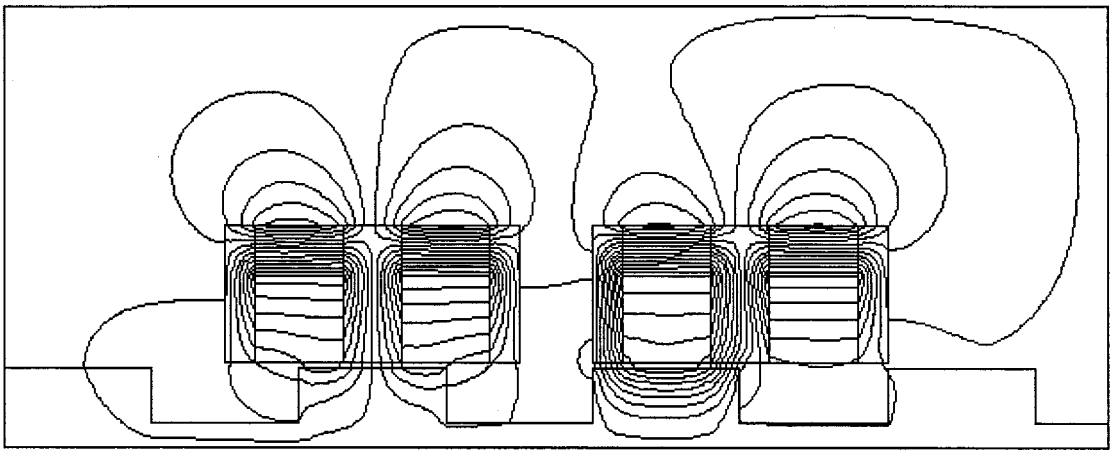

Fig. 5. Predicted no-load flux distribution.

are readily determined for regions such as the permanent magnets, the laminated stator poles, and the salient armature using the dimensional parameters defined in Fig. 1. However, the estimation of reluctances for the flux paths in air is somewhat more problematic, and necessarily reliant on a number of simplifications.

The change in flux linkage of the stator windings as the armature moves is the main figure of merit by which alternative generator designs can be compared. The peak-to-peak variation in flux linkage for one stator coil can be deduced using the lumped magnetic circuits shown in Fig. 3(a) and (b), which correspond to the salient poles of the armature being aligned and unaligned with the stator poles, respectively. With reference to Fig. 3, the various reluctance components can be calculated.

- S_g represents the air-gap reluctance due to the radial clearance between the surface of a salient pole on the armature and a stator pole. In the case of the unaligned position [Fig. 3(b)] it accounts for a small proportion of the total effective air-gap reluctance, whereas in the aligned position, it is the dominant component. Neglecting fringing and leakage fluxes, S_g is given by

$$S_g = \frac{l_g}{\mu_0 \pi r_i (l_\tau - l_m)}. \tag{1}$$

- S_{cl} represents the stator slot-leakage reluctance, which, for a parallel-sided slot, is determined from

$$S_{cl} = \frac{l_m}{\mu_0 \pi (r_m^2 - r_i^2)}. \tag{2}$$

- S_{va} is the nonlinear reluctance of the armature in the aligned position, and although it will generally be small compared to the air-gap component S_g, it is included in the lumped reluctance circuit since some generator designs may give rise to a high degree of saturation. The permeability μ_a is derived from the magnetization curve for the armature magnetic material and the armature flux density. Thus,

$$S_{va} = \frac{l_m + l_\tau}{2\pi \mu_a r_i^2}. \tag{3}$$

  Since the magnetization curve is nonlinear, the determination of μ_a necessitates an iterative solution of the lumped reluctance network.
- S_{vu1} represents the reluctance of the armature in the unaligned position, and is determined from

$$S_{vu1} = \frac{l_\tau}{\pi \mu_a r_c^2}. \tag{4}$$

- S_{vu2} represents the reluctance of the air space between the salient poles of the armature, and is given by

$$S_{vu2} = \frac{l_m + l_\tau}{2\pi \mu_0 \left[(r_i - l_g)^2 - r_c^2 \right]}. \tag{5}$$

- S_m represents the equivalent reluctance of the permanent magnet, which has a recoil permeability of μ_r. Thus,

$$S_m = \frac{l_m}{\mu_r \mu_0 \pi (r_e^2 - r_m^2)}. \tag{6}$$

- S_{il}—Since the stator poles are fabricated from annular laminations, the flux that results from the permanent magnet must cross a series of interlaminar gaps. If the lamination stacking factor is k_s, the equivalent reluctance is given by

$$S_{il} = \frac{(1 - k_s)(l_\tau - l_m)}{2\mu_0 \pi (r_e^2 - r_m^2)}. \tag{7}$$

- S_{et} represents the reluctance of the leakage flux paths from the outer surfaces of the stator poles. Assuming semicircular flux paths, the reluctance is given by [10]

$$S_{et} = \frac{l_\tau + l_m}{2\mu_0 r_e (l_\tau - l_m)}. \tag{8}$$

TABLE I
PARAMETERS OF PROTOTYPE GENERATOR

number of poles	4	number of phases	2
outer stator radius r_e	0.009 [m]	outer radius of magnets r_e	0.009 [m]
inner stator radius r_i	0.00344 [m]	inner radius of magnets r_m	0.007 [m]
airgap length l_g	0.00025 [m]	axial length of magnets l_m	0.0036 [m]
armature length	0.048 [m]	pole-pitch l_τ	0.006 [m]
number of turns per phase	2 x 3100	capacitance	68 μf / 25V
wire diameter	0.050 [mm]		

TABLE II
COMPARISON OF LUMPED CIRCUIT AND FINITE-ELEMENT METHOD COMPARISON TECHNIQUE

Analysis technique	Flux variation [mWb]
Lumped magnetic circuit	0.0684
Finite Element Analysis	0.0713

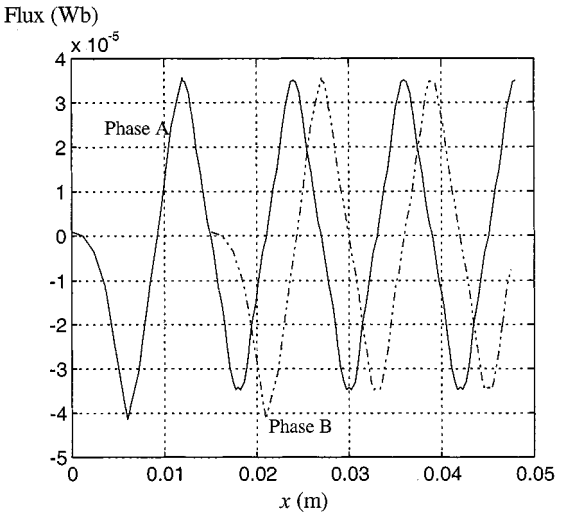

Fig. 6. Finite-element predicted flux as a function of armature position.

- $S_{\rm em}$ represents the reluctance to leakage flux from the permanent magnet, and is given by

$$S_{\rm em} = \frac{1}{2\mu_0 r_e}. \tag{9}$$

- S_{t1} and S_{t2} represent the reluctance of the stator poles in the radial direction. Again, these will only be significant if the degree of saturation is significant

$$S_{t1} = \frac{r_m - r_i}{\pi\mu_0[r_r + 0.5(r_m + r_i)](l_\tau - l_m)} \tag{10}$$

$$S_{t2} = \frac{2(r_e - r_i)}{\pi\mu_0(r_e + 3r_i)(l_\tau - l_m)}. \tag{11}$$

- F_m is the magnetic-motive force of the permanent magnet, and is given by

$$F_m = \frac{B_{\rm rem}}{\mu_0\mu_r} l_m \tag{12}$$

where $B_{\rm rem}$ is the remanence.

By solving the lumped magnetic circuits corresponding to the aligned and unaligned armature positions, the fluxes in the various regions can be estimated. Of particular interest, in terms of the generator performance, is the flux that links the winding

$$\Phi = \Phi_g + \frac{\Phi_c}{2} \tag{13}$$

where Φ_g is the air-gap flux which passes through S_g, and Φ_c is the leakage flux which passes through S_{cl}. From the calculated flux for both the unaligned and aligned armature positions, the maximum flux change $\Delta\Phi$ can be calculated. Thus, the average induced voltage e in the two coils which form a phase winding during the period in which the armature is displaced one pole pitch is given by

$$e = \frac{2N\Delta\Phi}{\Delta t} = \frac{2Nv\Delta\Phi}{l_\tau} \tag{14}$$

where N is the number of turns per coil and v is the armature velocity. The output power generated by one pole pair is, therefore, given by

$$P_{\rm em} = EI = \frac{2N\Delta\Phi v I}{l_\tau} \tag{15}$$

where the winding current I is related to the current density J, the winding packing factor k_p, and the stator slot area $(r_m - r_i) \cdot l_m$ by

$$I = \frac{Jk_p l_m (r_m - r_i)}{N}. \tag{16}$$

Substituting (16) into (15) yields

$$P_{\rm em} = \frac{2vJk_p\Delta\Phi (r_m - r_l) l_m}{l_\tau}. \tag{17}$$

Therefore, the electromagnetic thrust force $F_{\rm em}$ is given by

$$F_{\rm em} = \frac{P_{\rm em}}{v} = \frac{2Jk_p\Delta\Phi (r_m - r_i) l_m}{l_\tau}. \tag{18}$$

Equation (18) relates the thrust force capability to the generator design parameters and facilitates design optimization by scanning critical design parameters so as to maximize the force, a procedure which is particularly rapid with the lumped equivalent circuit analysis technique. By means of example, Fig. 4 shows the variation of $F_{\rm em}$ as a function of the dimensional ratios r_i/r_e and lm/l_τ, assuming $B_{\rm rem} = 1.2$ T, $\mu_r = 1.05$, $r_e = 0.009$ m, $r_m = 0.007$ m, $l_\tau = 0.006$ m, $l_g = 0.000\,25$ m.

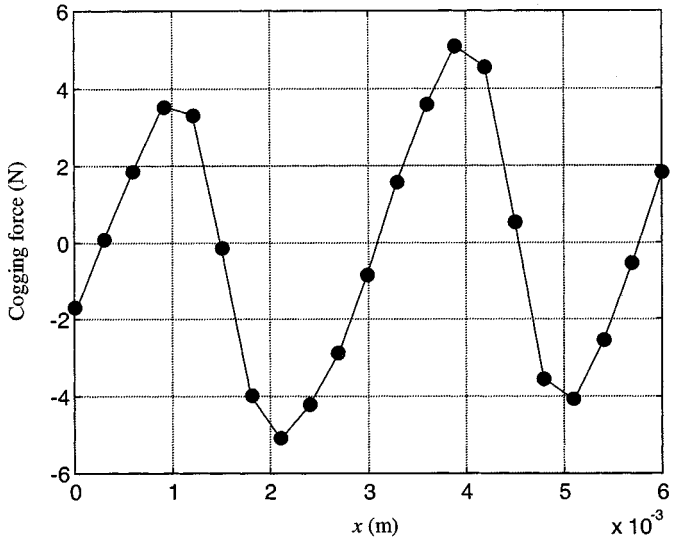

Fig. 7. Variation of cogging force as a function of armature position.

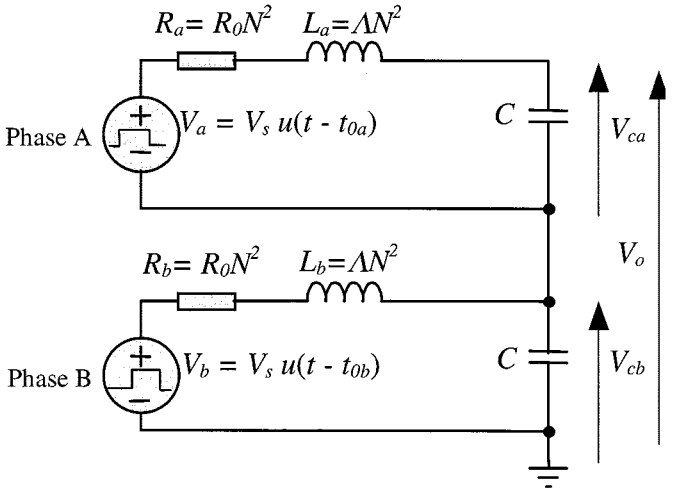

Fig. 9. Simplified rectification end energy storage circuit.

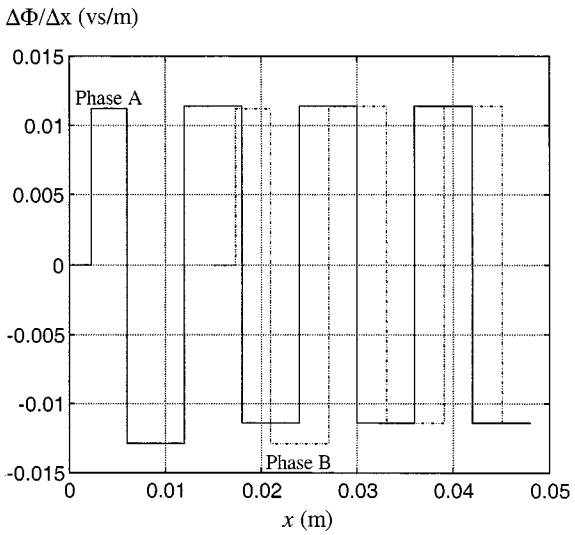

Fig. 8. Rate of change of flux with respect to displacement of armature.

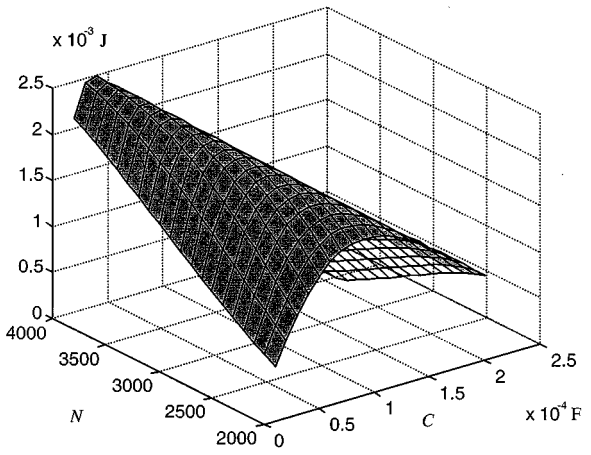

Fig. 10. Output energy as a function of N and C.

As is evident from Fig. 4, an optimum combination of dimensional parameters exists which yields the maximum thrust force, i.e., $r_i/r_e = 0.375$, $l_m/l_\tau = 0.6$.

B. Finite-Element Analysis

Although the lumped magnetic circuit analysis is useful for identifying likely optimal designs, it makes simplifying assumptions regarding the dominant flux paths, which are themselves dependent on the particular combination of generator design parameters. Thus, it is prudent to perform a more detailed analysis of the magnetic field distribution using magneto-static finite-element analysis. By way of illustration, Fig. 5 shows no-load field distribution of a two-phase generator having the parameters listed in Table I, which conform to the optimal ratios for r_i/r_e and l_m/l_τ, established in Fig. 4. Table II compares the predicted change in flux linking a stator coil when the armature is moved from an aligned to an unaligned position. As will be seen, the prediction from the lumped magnetic circuit agrees reasonably with that from finite-element analysis.

The optimal design parameters which were derived from the lumped magnetic circuit analysis, i.e., $r_i/r_e = 0.375$ and $l_m/l_\tau = 0.6$, were validated using finite— element analysis by slightly varying the ratios and computing the performance. However, this merely confirmed that the optimal values were correct. Further finite-element analysis was undertaken in order to evaluate the generator performance in greater detail, specifically, the variation of the winding flux linkages, self-inductances, and cogging force with armature position. Fig. 6 shows the variation of winding flux-linkages for the two phases as the armature traverses a complete stroke of 48 mm, while Fig. 7 shows the variation of cogging force over the initial 5 mm of the stroke (where $x = 0$ in both figures corresponds to the position when the armature tip is about to enter the stator).

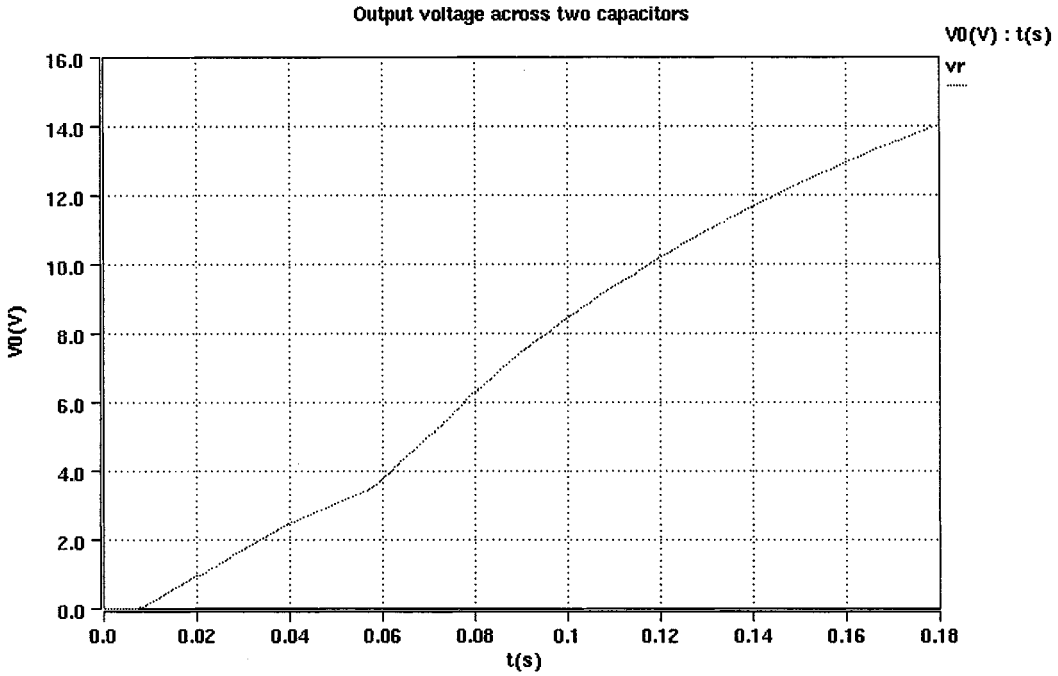

Fig. 11. Output voltage.

III. Winding Design and Rectifier/Capacitor Circuit

The design of the phase windings, i.e., the selection of the number of turns and, hence, the conductor diameter, is closely coupled to the selection of the rectifier and capacitor system for the energy storage. Thus, a system-level approach embracing the electromagnetic design aspects and the electrical circuit parameters must be employed.

The winding resistance and self-inductance per phase can be expressed in terms of a normalized resistance R_0 and a normalized inductance Λ, i.e,

$$R_w = R_0 N^2 \tag{19}$$

$$L_s = \Lambda N^2 \tag{20}$$

where R_0 is constant for a particular combination of dimensions r_m, r_i and l_m, and is given by

$$R_0 = \frac{2\rho\,(r_m + r_i)}{k_p\,(r_m - r_i)\,l_m} \tag{21}$$

and ρ is the resistivity of copper at 20 °C ($1.78 \times 10^{-8}\ \Omega$m).

The normalized self-inductance Λ, corresponds to the effective permeance associated with the coil flux, and can be determined from finite-element analysis. It is a function of the relative position of the armature and stator poles. However, finite-element analysis shows that for the generator having the parameters given in Table I, the variation of Λ over a complete stroke is less than 20%, having a maximum value of 0.954 H and a minimum value of 0.847 H. This relative insensitivity to armature position is due to the fact that a permanent magnet with a recoil permeability which is close to μ_0 is situated in the main flux path of the coils, and that a significant proportion of the self-inductance is due to the "slot-leakage" flux component. Thus, Λ can be assumed to have a constant magnitude, equal to the average value over the stroke, which considerably simplifies the optimization of the coil design and the choice of the energy storage capacitor. It will be noted that the mutual inductance between the two phases is essentially zero, and can be neglected.

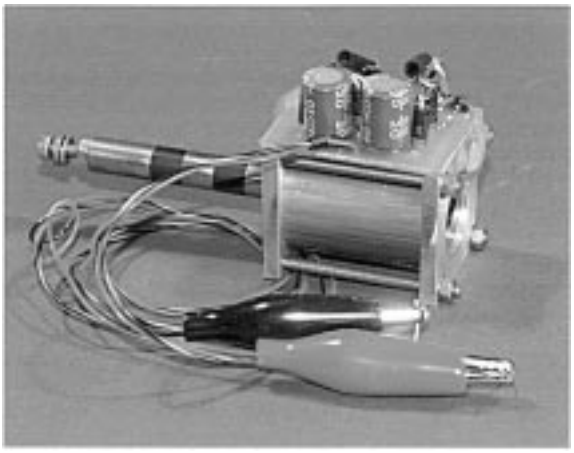

Fig. 12. Prototype generator.

From the results shown in Fig. 6, the rate of change of flux with displacement of the armature approximates to a square waveform, as shown in Fig. 8. This, in turn, allows the EMF per turn to be calculated. By modeling the rectifier diodes as ideal devices with a fixed voltage drop ΔV_d, the rectifier and capacitor circuit of Fig. 2 can be simplified to the equivalent circuit shown in Fig. 9, which comprises two R–L–C circuits excited by two independent voltage sources. On the basis of the square flux linkage waveforms shown in Fig. 8, the amplitude of the two voltage sources, V_s, are given by

$$V_s = K_e N - 2\Delta V_d \tag{22}$$

TABLE III
MEASURED AND PREDICTED WINDING RESISTANCE AND INDUCTANCE

	Resistance (Ω at 20 C^0)		Inductance (H)			
	predicted	measured	Minimum value		Maximum value	
			predicted	measured	predicted	measured
Phase A	1787	1741	0.846	0.758	0.954	0.866
Phase B	1787	1748	0.846	0.774	0.954	0.883

where $K_e = [\Delta\Phi/\Delta x]_m \cdot v$ and $[\Delta\Phi/\Delta x]_m$ is the magnitude of $\Delta\Phi/\Delta x$ shown in Fig. 8.

The two voltage-source R–L–C circuits in Fig. 9 are decoupled, and hence, can be solved independently. If the armature moves at a speed v for a time duration of T_e, and the two phase EMF waveforms are initiated at instants of time t_{0a} and t_{0b}, then the resultant voltages across the capacitors at $t = T_e$ are given analytically by (23), from which it is evident that the capacitor voltage is a function of both N and C

$$V_{ci}|_{t=T_e} = L^{-1}\left\{\frac{K_E N - 2\Delta V_d}{(C\Lambda N^2 s^2 + R_0 N^2 s + 1)s}\right\}\Bigg|_{t=T_e - t_{0i}}, \quad i = a, b. \tag{23}$$

If the output voltage is regulated by a voltage regulator which requires a minimum voltage of 5.6 V to provide a stable output of 5 V, then the total energy which is available when the two capacitors are subsequently discharged is given by

$$E_{ct} = 0.25C\left[(V_{ca} + V_{cb})^2 - 5.6^2\right]. \tag{24}$$

Equations (23) and (24) relate the output energy of the generator-power conditioning circuit to the design parameters N and C. By scanning these two parameters between specified limits, optimal values can be identified which result in maximum stored energy for a specified motion of the armature. Fig. 10 shows the variation of the output energy as a function of N and C, calculated using (23) and (24), assuming an armature velocity v of 0.3 m s^{-1}. Clearly, for a given value of N, there is an optimal value for C which yields maximum stored energy E_{ct}. As the number of turns N is progressively increased, the optimal value of C decreases while the maximum output energy E_{ct} increases. However, for values of N greater than 3000, the increase in E_{ct} is no longer significant, while the required wire diameter becomes impracticably small.

The validity of this foregoing analysis has been verified by a more rigorous simulation of the generator–rectifier–capacitor system shown in Fig. 2 using the simulation package Saber. By way of example, Fig. 11 shows how the voltage across the two capacitors varies with time for the case of $N = 3100$, $C = 68\ \mu$F and a constant armature velocity of 0.3 m s^{-1}. The energy that is recoverable by discharging the capacitors is 2.7 mJ, after which the output voltage drops to 5.6 V, which is in reasonable agreement with the analytically derived value of 2.4 mJ. A significant proportion of the difference may be attributed to the nonlinear behavior of the diodes, which is not accounted for in (23).

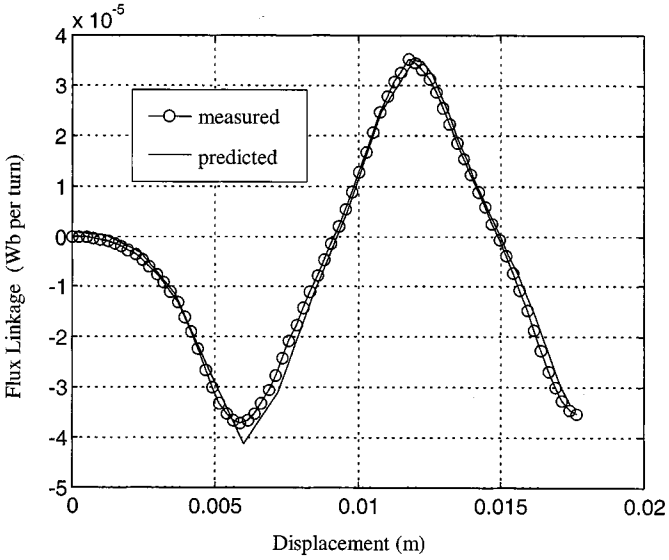

Fig. 13. Flux-linkage of phase *A* as a function of armature displacement.

IV. EXPERIMENTAL RESULTS

A prototype generator having the design parameters given in Table I is shown in Fig. 12. The measured and predicted winding resistance and inductance compare favorably as shown in Table III. The measured and predicted flux linkage of phase *A* as a function of armature displacement are compared in Fig. 13, with zero displacement corresponding to the armature tip entering the stator. Fig. 14 shows typical measured capacitor voltage waveforms and the associated armature velocity waveforms, derived from a linear incremental encoder, during a single stroke of armature. As is evident from these results, the system is capable of producing an output voltage of 12–16.5 V, for average armature velocities ranging from 0.15 to 0.45 m s^{-1}. The resulting stored energy varies from 2.45 to 4.63 mJ, which meets the target performance specification. It will also be observed that, due to the presence of cogging force, the armature velocity fluctuates significantly during the stroke, particularly at lower speeds.

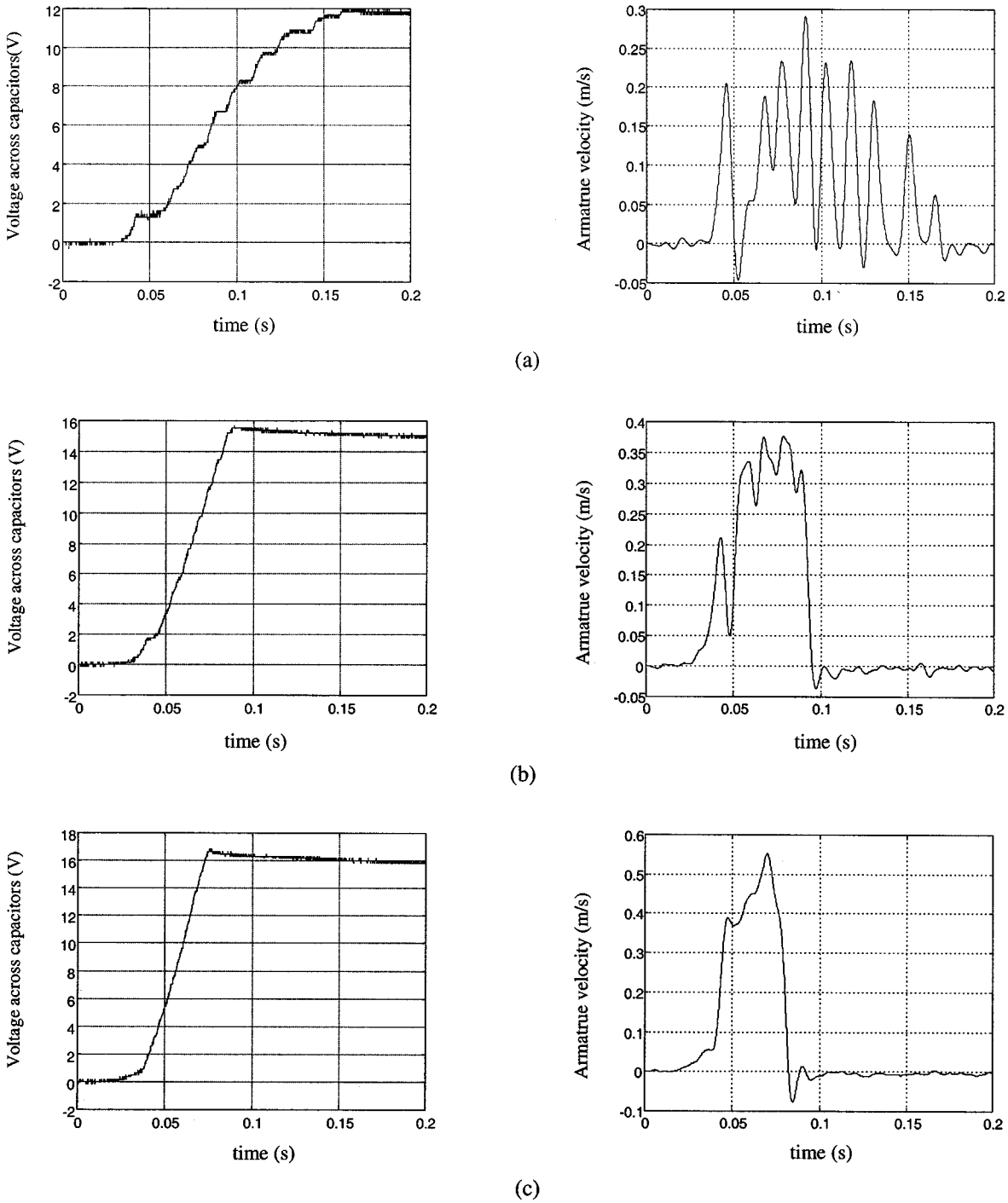

Fig. 14. Measured capacitor voltage and armature velocity waveforms during a single stroke of armature. (a) Average armature velocity $= 0.15$ m s^{-1}. (b) Average armature velocity $= 0.30$ m s^{-1}. (c) Average armature velocity $= 0.45$ m s^{-1}.

V. Conclusions

This paper has described the design, analysis, and experimental characterization of a tubular permanent-magnet generator and an associated power conditioning circuit. The merits of combining lumped magnetic circuit analysis and finite-element analysis to optimize the design of the generator has been illustrated, and the need for system-level analysis to concurrently design the winding and select the energy storage capacitors has been highlighted. Performance predictions agree well with experimental results from a prototype generator.

References

[1] C. B. Williams and R. B. Yates, "Analysis of a micro-electric generator for microsystems," *Sens. Actuators*, vol. A52, pp. 8–11, 1996.

[2] J. Wang, W. Wang, G. W. Jewell, and D. Howe, "Design and experimental characterization of a linear reciprocating generator," *Proc. IEE—Electric Power Applicat.*, vol. 145, no. 6, pp. 509–518, 1998.

[3] ——, "Analysis and design of a linear reciprocating generator for telemetry-based vibration monitoring system," in *Proc. ICEM'98*, 1998, pp. 857–862.
[4] J. Wang, G. W. Jewell, and D. Howe, "A general framework for the analysis and design of tubular linear permanent magnet machines," *IEEE Trans. Magn.*, vol. 35, pp. 1986–2000, May 1999.
[5] B. Lequesne, "Permanent magnet linear motors for short strokes," *IEEE Trans. Ind. Applicat.*, vol. 32, pp. 161–168, Jan./Feb. 1996.
[6] White, K. Colenbrander, R. W. Olan, and L. B. Penswick, "Generators that won't wear out," *Mech. Eng.*, vol. 118, no. 2, pp. 92–96, 1996.
[7] M. Watada, K. Yamashima, Y. Oishi, and D. Ebihara, "Improvement of characteristics of linear oscillatory actuator for artificial hearts," *IEEE Trans. Magn.*, vol. 29, pp. 3361–63, Nov. 1993.
[8] M. K. Jenkins, G. W. Jewell, K. Harmer, and D. Howe, "Design of a micro-generator for a smart-diskette," in *Proc. 12th Int. Workshop Rare Earth Magnets and Their Applications*, 1992, pp. 121–132.
[9] P. J. Hor, Z. Q. Zhu, D. Howe, and J. Rees-Jones, "Minimization of cogging force in a novel linear brushless permanent magnet motor," in *Proc. IEEE Compumag Conf.*, 1997, pp. 345–346.
[10] Z. Q. Zhu and D. Howe, "Magnet design considerations for electrical machines equipped with surface-mounted permanent magnets," in *Proc. 13th Int. Workshop Rare-Earth Permanent Magnets Applications*, 1994, pp. 151–160.

Jiabin Wang (M'96) was born in Jiangsu Province, China, in 1958. He received the B.Eng. and M.Eng. degrees from Jiangsu University of Science and Technology, Zhengjiang, China, and the Ph.D. degree from the University of East London, London, U.K., in 1982, 1986, and 1996, respectively, all in electrical and electronic engineering.

From 1986 to 1991, he was with the Department of Electrical Engineering, Jiangsu University of Science and Technology, where he was appointed a Lecturer in 1987 and an Associate Professor in 1990. He was a Post-Doctoral Research Associate at the University of Sheffield,Sheffield, U.K., from 1996 to 1997 and a Senior Lecturer at the University of East London from 1998 to 2001. He is currently a Senior Lecturer at the University of Sheffield. His research interests range from motion control to electromagnetic devices and their associated drives.

Weiya Wang was born in Jiangsu Province, China, in 1957. She received the B.Eng. degree from Jiangsu University of Science and Technology, Zhengjiang, China, and the M.Sc. degree from the University of East London, London, U.K., in 1982 and 1996, respectively, both in electrical and electronic engineering.

From 1982 to 1993, she was with the Department of Electrical Engineering, Jiangsu University of Science and Technology, where she was appointed a Lecturer in 1988. She was a Research Associate at the University of Sheffield from 1997 to 1998 and is currently a Senior Research Fellow at Anglia Polytechnic University, Chelmsford, U.K. Her research interests include electromagnetic devices, miniature mobile robots, meta-level learning, and electronic learning.

Geraint W. Jewell was born in Neath, U.K., in 1966. He received the B.Eng and Ph.D. degrees from the Department of Electronic and Electrical Engineering, University of Sheffield, Sheffield, U.K., in 1988 and 1992, respectively.

From 1994 to 2000, he was a Lecturer in the Electrical Machines and Drives Research Group, University of Sheffield, where he currently holds an Engineering and Physical Sciences Research Council Advanced Research Fellowship. His research interests cover many aspects of both permanent-magnet and reluctance-based electrical machines and actuators.

David Howe received the B.Tech and M.Sc. degrees from the University of Bradford, Bradford, U.K., and the Ph.D. degree from the University of Southampton, Southampton, U.K., in 1966, 1967, and 1974, respectively, all in electrical power engineering.

He has held academic posts at Brunel and Southampton Universities, and spent a period in industry with NEI Parsons Ltd., working on electromagnetic problems related to turbogenerators. He is currently a Professor of Electrical Engineering at the University of Sheffield, Sheffield, U.K., where he heads the Electrical Machines and Drives Research Group. His research activities span all facets of controlled electrical drive systems, with particular emphasis on permanent-magnet excited machines.

Prof. Howe is a Chartered Engineer in the U.K. and a Fellow of the Institution of Electrical Engineers, U.K.